



Stabilizing lithium/sulfur batteries by a composite polymer electrolyte containing mesoporous silica particles



Kazem Jедди^a, Kaveh Sarikhani^a, Nader Taheri Qazvini^b, P. Chen^{a,*}

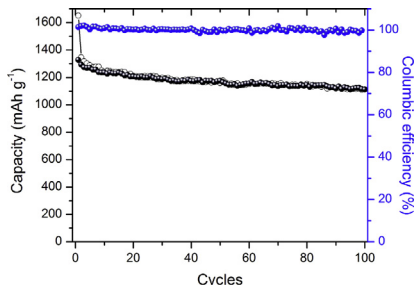
^aWaterloo Institute for Nanotechnology, Department of Chemical Engineering, University of Waterloo, 200 University Avenue West, Waterloo, Ontario, Canada N2L3G1

^bPolymer Division, School of Chemistry, College of Science, University of Tehran, P.O. Box 14155-6455, Tehran, Iran

HIGHLIGHTS

- Mesoporous silica particles were synthesized by a simple sol–gel procedure.
- A composite polymer electrolyte was fabricated and utilized in Li/S batteries.
- The resultant Li/S battery exhibited a high initial capacity of 1648 mA h g⁻¹.
- This Li/S battery also demonstrated an excellent cycling performance.
- Discharge capacity of 1143 mA h g⁻¹ was obtained after more than 100 cycles.

GRAPHICAL ABSTRACT



ARTICLE INFO

Article history:

Received 10 March 2013
Received in revised form
25 June 2013
Accepted 26 June 2013
Available online 4 July 2013

Keywords:
Energy storage
Lithium/sulfur battery
Polymer electrolyte
Polysulfide dissolution

ABSTRACT

Development of lithium/sulfur (Li/S) batteries is limited by their low Coulombic efficiency and low cycle life, which are mainly due to active mass loss and polysulfide dissolution into the electrolyte solution. Here we report a new approach to overcome these drawbacks by employing a novel composite polymer electrolyte that not only facilitates rapid transport of lithium ions for electrochemical reactions with sulfur, resulting in improved capacity of the battery, but also prevents the generated polysulfides from shuttling between the electrodes during cycling of the battery. Improved performance of the battery was achieved: An initial discharge capacity of 1648 mA h g⁻¹ and reversible capacity of 1143 mA h g⁻¹ sulfur were obtained after 100 cycles at 0.2 C (1 C = 1672 mA h g⁻¹), which could be among the highest reversible capacities reported for Li/S batteries so far.

© 2013 Elsevier B.V. All rights reserved.

1. Introduction

Sulfur is a promising cathode material for rechargeable lithium batteries due to its high theoretical specific capacity of 1672 mA h g⁻¹ and specific energy of 2600 W h kg⁻¹, when the complete reaction of lithium with sulfur is assumed [1,2]. Such a

high specific energy is 3–5 times higher than that of the conventional rechargeable lithium ion batteries based on intercalation chemistry [3]. The relatively low operating voltage of about 2.1 V compared to 3.0–4.0 V of other cathode materials can assure better safety of the battery package. Moreover, sulfur is abundant, non toxic, and can be used to produce cheap and safe high-energy batteries [4,5].

In spite of these advantages, a few challenges have prevented practical application of Li/S batteries so far. One of the major issues is the poor cyclability, which is mainly due to the high solubility of

* Corresponding author. Tel.: +1 519 888 4567x35586; fax: +1 519 746 4979.
E-mail address: p4chen@uwaterloo.ca (P. Chen).

the lithium polysulfides produced during cycling into the liquid electrolyte solution [6,7]. These intermediate products can shuttle between the electrodes, going through a few reduction reactions at the anode and oxidation reactions at the cathode. Consequently, some of the soluble polysulfides are reduced to insoluble intermediate species that can be deposited on the anode and the cathode surfaces during charge and discharge processes [8]. This phenomenon finally results in increased impedance of the cell, degradation of the electrode structure, and more importantly, active mass loss due to inaccessibility of the active components in the electrode [9]. The combination of these effects can decrease the Coulombic efficiency and accelerate the capacity fading of Li/S batteries.

Extensive research has been conducted to improve the discharge capacity retention and Coulombic efficiency of Li/S batteries. In order to reduce the polysulfide dissolution, some recent studies have focused on developing solid polymer electrolytes (SPEs) and gel polymer electrolytes (GPEs) as alternatives to the conventional liquid electrolytes. Poly (ethylene oxide) (PEO) based electrolytes have been considered an appropriate SPE candidate to achieve a solid-state Li/S battery configuration. However, the crystalline structure of PEO severely suppresses the ionic conductivity at ambient condition. Therefore, the application of these batteries is limited to temperatures above the melting point of PEO ($\sim 63^\circ\text{C}$), at which sufficiently high ionic conductivity ($\sim 10^{-3} \text{ S cm}^{-1}$) is obtained [10]. Gel polymer electrolytes (GPEs), which consist of solid matrices that provide mechanical strength and embedded liquid electrolytes responsible for electrochemical properties, seem to be a better alternative in Li/S batteries [11–13]. However, GPEs lose their mechanical stability after liquid electrolyte uptake, leading to poor compatibility with the lithium anode which can cause serious problems in terms of battery safety and cyclability [14]. More importantly, poor liquid electrolyte upholding of the GPE facilitates lithium polysulfide dissolution after a few cycles, hence accelerating performance fading in Li/GPE/S cells [15].

A promising path to overcome this dilemma and consequently achieve better electrolytes for Li/S batteries may be fabrication of

GPEs that allow facile transport of Li^+ ions but prevent diffusion of polysulfides to suppress shuttle phenomenon [16–18]. In this communication, we propose a composite gel polymer electrolyte comprising a polymer matrix and mesoporous silica particles to improve the cyclability of Li/S batteries. Such an electrolyte, which is a liquid electrolyte immobilized in the porous composite membrane, potentially offers at least two unique characteristics. First, it can provide immobilizing electrolyte solution within the composite structure during cycling of the battery. Second, the nanometer-sized particles form a porous mesh that provides a path for lithium ions, but prevents the intermediate products from shuttling between electrodes.

2. Experimental

2.1. Material preparation

Mesoporous silica (MPS) particles were synthesized by a simple procedure, as shown in Fig. 1 [19]. Brij 56, a nonionic surfactant, was dissolved in a dilute HCl solution ($\text{pH} = 1.5$). Then, tetramethyl orthosilicate (TMOS) was added to the solution with mild stirring at room temperature. After 20 min, the homogenous and transparent solution was poured into a Teflon dish. After two days, a glassy monolith sample was obtained and dried at $40\text{--}100^\circ\text{C}$ in a vacuum oven for 24 h to remove all the residual solvents. Finally, the surfactant was removed by calcinations in air atmosphere at 550°C for 16 h.

A functional poly(methyl methacrylate) (f-PMMA) was synthesized by free radical polymerization of methylmethacrylate (MMA) (0.1 mol) and methacryloxypropyltrimethoxysilane (MPTMS) (10 mmol) in tetrahydofuran (THF) using AIBN as the initiator following a procedure described in our previous work [17]. MPS, poly(vinylidene fluoride-co-hexafluoropropylene) (PVdF-HFP) and f-PMMA were dissolved in acetone by mechanical stirring overnight. This step was followed by ultrasonication for 1 h to form a homogenous solution at room temperature. Then, tert-butyl methyl ether was added and this mixture was left agitating until

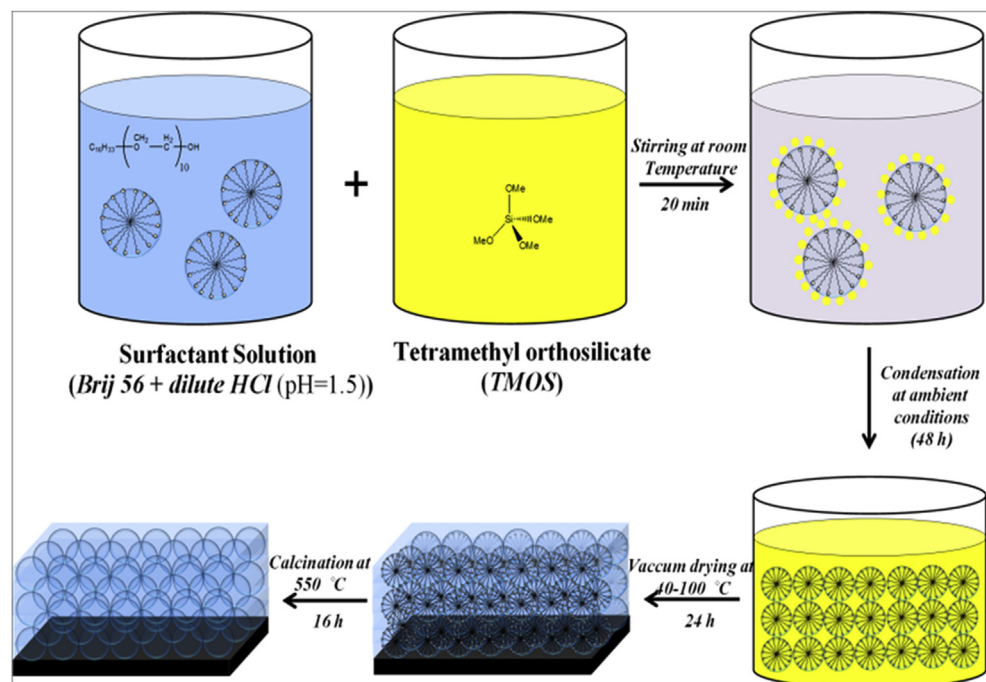


Fig. 1. Schematic of the synthesis steps for mesoporous silica particles.

the solution was homogenous. The resulting solution was poured onto a clean petri dish. After evaporation of acetone and ether, the electrolyte membrane was further dried at 65 °C in a vacuum oven for 24 h to remove any traces of the acetone and ether. The polymer electrolyte was finally obtained by soaking the membrane in 1 M LiPF₆ dissolved in a 1:1 (v/v) mixture of ethylene carbonate (EC) and diethylene carbonate (DEC) for 30 min. Hereafter, we refer to the composite polymer electrolyte with the acronyms CPE.

Sulfur/polyacrylonitrile (S/PAN) composite was chosen to be used as the cathode material. It has been reported that sulfur can either be distributed homogeneously in the conductive PAN or can bind to the PAN matrix chains during the heat treatment. This would result in significant improvements of Li/S battery performance in terms of specific capacity and cyclability [20–22]. However, the electrochemical properties of S/PAN composite cathodes are highly dependent on the preparation procedure. In order to obtain a good S/PAN cathode, reaction between sulfur and PAN is necessary during heat treatment. This can be classified in three different temperature ranges:

- 1) Below 280 °C there would be no reaction between S and PAN. Sulfur remains in its elemental state (agglomerated poly (sulfur)). As a result a very poor electrochemical performance is obtained [23].
- 2) Between 280 and 450 °C reaction occurs between sulfur and PAN, obtaining a composite that contains amorphous sulfur (nano-sulfur) distributed within the conductive polymer matrix, and also polymer chains with S–S_x (0 < x < 6) bonds at side chains [21,24]. This composite shows high initial capacities, but the capacity reduces upon cycling due to lower

electric conductivity of sulfur and formation of lithium polysulfides that are soluble in liquid electrolyte (polysulfide shuttle) [9,20].

- 3) Above 450 °C a complete reaction between sulfur and PAN and formation of a disulfur side-chain functioning in the electrochemical reactions. As a result, excellent cyclability but low capacity are achieved [21].

In this study, the composite cathode was prepared by ball milling the mixture of sulfur (Sigma–Aldrich) and PAN (Sigma–Aldrich) in a weight ratio of 3:1. This process was followed by heat treatment at 300 °C for 3 h in a tubular furnace filled with Ar gas. The amount of active material in the heat-treated S/PAN composite was 42%. The final sulfur-based cathode material was then prepared by mixing 80 wt% of S/PAN composite, 10 wt% acetylene black (99.5% purity, MTI), and 10 wt% PVdF (Kynar, HSV900) dissolved in N-methyl-2-pyrrolidene (NMP) (\geq 99.5% purity, Sigma–Aldrich). The sulfur mass loading of the electrode was about of 2 mg cm⁻².

2.2. Characterization of the materials

The morphology of the samples was investigated by using field emission scanning electron microscopy (FE-SEM) (Leo-1530, Zeiss). The samples were gold-sprayed prior to SEM measurements. Nitrogen adsorption/desorption isotherms were measured at 77 K with a surface area analyzer (ASAP 2020). Prior to the measurements, the samples were degassed at 300 °C for at least 24 h. The Brunauer–Emmett–Teller (BET) method was used to calculate the specific surface area. The Barrett–Joyner–Halenda (BJH) model was also used to calculate the pore size and volume. The

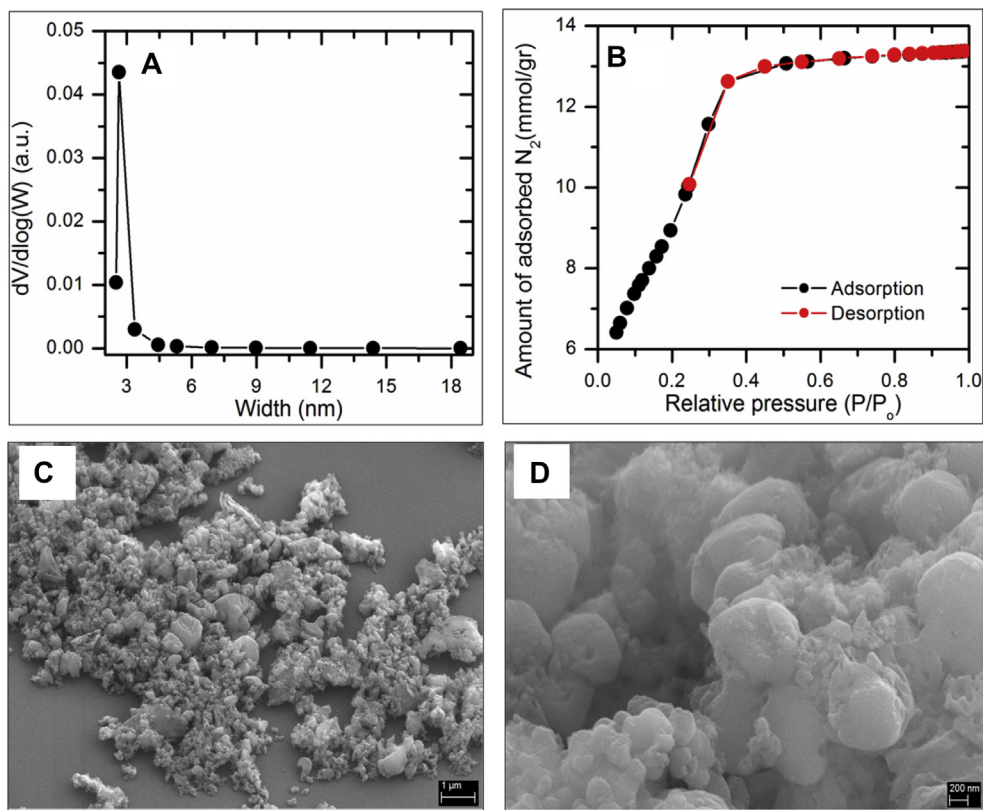


Fig. 2. Characterization of the synthesized particles; (A) nitrogen adsorption/desorption isotherm, (B) BJH pore size distribution graphs, (C) and (D) SEM images at low and high magnifications.

electrochemical properties were investigated using coin-type cells (CR2032) with a lithium metal anode, a sulfur-based cathode and the composite polymer electrolyte. A Li/S battery cell with liquid electrolyte (a polypropylene separator (Celgard, USA) with 1 M LiPF₆ dissolved in 1:1 (v/v) mixture of EC and DEC) was also prepared to be used as a control sample. AC impedance spectroscopy was performed on the Li/S batteries cells with a potentiostat (VMP3, BioLogic) over the frequency range from 0.1 Hz to 1 MHz at room temperature. The cycling performance of the cells was investigated at room temperature on an Arbin BT2000 battery testing system in galvanostatic mode with cut-off voltages of 1.0 V and 3.0 V.

3. Results and discussion

Fig. 2(A) and (B) shows the pore size distribution and the nitrogen adsorption/desorption isotherm curves of the MPS particles. The synthesized particles had the following properties: a BET surface area of 804.15 m² g⁻¹, pore volume of 0.86 cm³ g⁻¹, and pore size of 3.83 nm. The scanning electron microscopy (SEM) images of the MPS particles at two different magnifications are shown in **Fig. 2(C) and (D)**. These images reveal that the synthesized silica is composed of spherical particles with diameters of between 200 and 400 nm, with no strict long-range order.

Scanning electron microscopy images for the composite polymer membrane are shown in **Fig. 3**. The electrolyte membrane has a thickness of about 100 μm. As can be seen, a porous membrane with small and uniformly distributed pores was obtained which would improve the electrolyte solution uptake and promote stability of the GPE morphology during cycling. Moreover, small and uniformly distributed pores might increase the mechanical stability of the polymer electrolyte.

Fig. 4 presents the Nyquist plots of these battery cells obtained from AC impedance spectroscopy at the end of each cycle (i.e., end of the charge process) illustrating their impedance trends upon cycling. Both cells exhibit low bulk (ohmic) resistance indicating the ease of lithium ion transportation within these cells. Furthermore, both fresh cells exhibit a high charge transfer resistance, which remarkably decreases upon initial cycling. In the case of Li/liquid electrolyte/S cell, a stable charge transfer resistance is observed after second cycle. But, the Li/CPE/S cell shows higher charge transfer resistance, compared to the other cell that consistently increases upon cycling. This trend in charge transfer resistance of the Li/CPE/S cell is attributed to its slow reaction kinetics. In this case, diffusion of the generated polysulfides through the electrolyte membrane is hindered, resulting in accumulation of these intermediate products in the cathode area and slowing the electrochemical reactions during cycling [17].

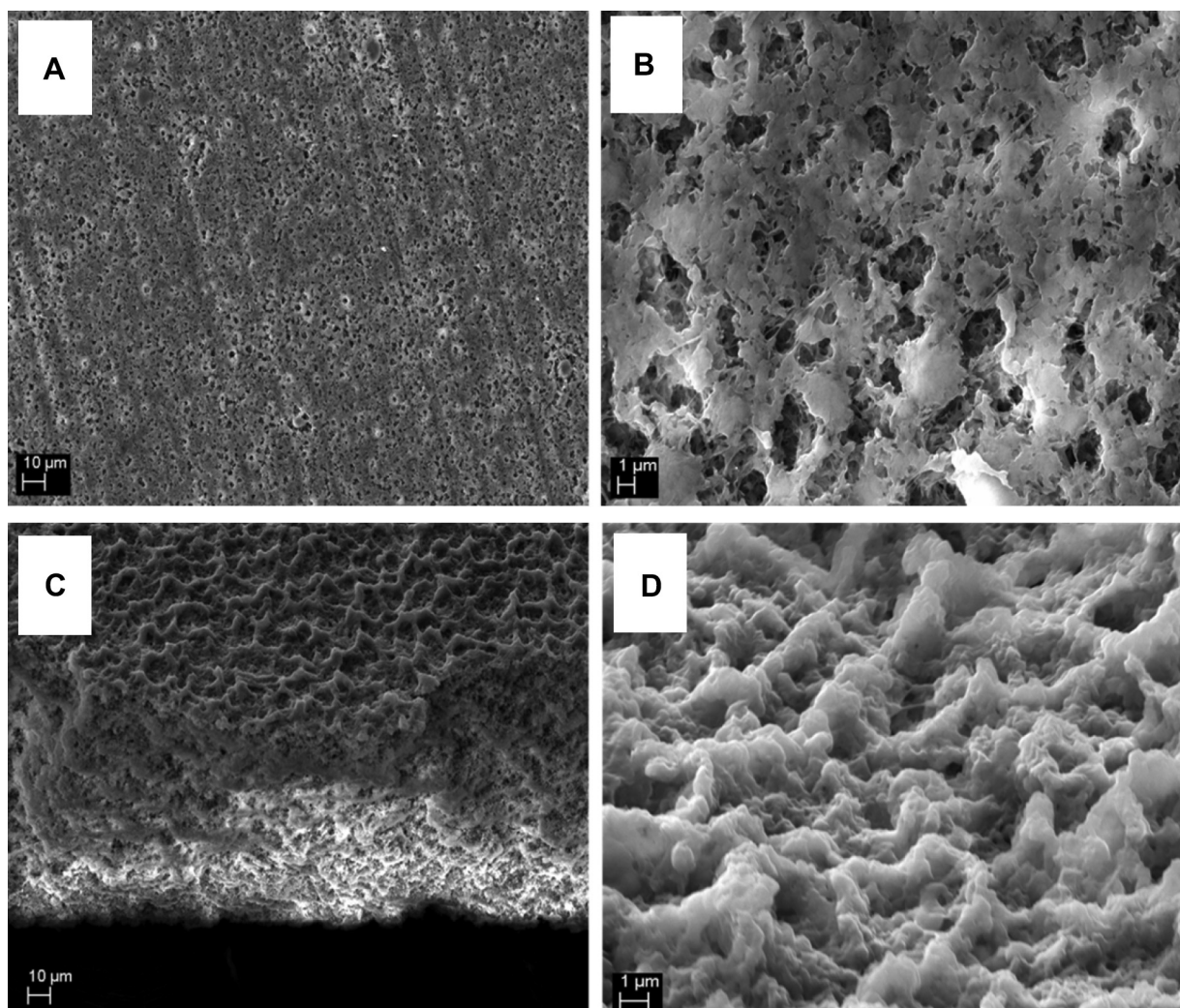


Fig. 3. SEM images of the surface and cross-section of the composite polymer electrolyte.

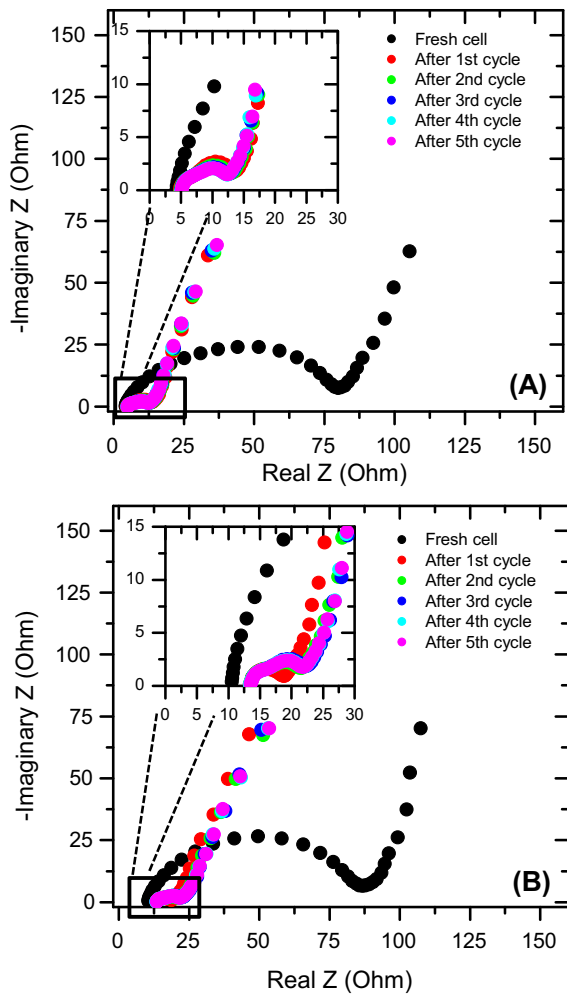


Fig. 4. Complex impedance plots for the first few cycles of (A) Li/liquid electrolyte/S and (B) Li/CPE/S battery cells.

Fig. 5 shows some galvanostatic charge/discharge cycles for both Li/S cells. The Li/liquid electrolyte/S exhibits an initial discharge capacity of 1610 mA h g^{-1} and initial charge capacity of about 1300 mA h g^{-1} based on the weight of sulfur active material. These values for the Li/CPE/S are 1648 mA h g^{-1} and 1277 mA h g^{-1} , respectively. Achieving such a high initial capacity values indicate complete reaction between lithium and sulfur, which is due to high ionic conductivity in both of the electrolytes used in these batteries, which supplies sufficient lithium ions for further electrochemical reactions with sulfur and results in the improved capacity of the cell [25]. **Fig. 6** presents discharge capacity versus cycle number for these battery cells. As can be seen, the Li/liquid electrolyte/S cell exhibits a stable cyclability up to 40 cycles. Then, poor cyclability leads to a low capacity of about $400 \text{ mA h g}_{\text{sulfur}}^{-1}$ or $135 \text{ mA h g}_{\text{composite}}^{-1}$ after 100 cycles. The active mass loss due to the dissolution of polysulfides into electrolyte solution and diffusion of these polysulfides through the separator (shuttle effect) is the main reason of such poor capacity retention in the Li/liquid electrolyte/S cell [17]. In contrast, the Li/CPE/S battery cell exhibits remarkably better capacity retention; a discharge capacity of $1143 \text{ mA h g}_{\text{sulfur}}^{-1}$ or $385 \text{ mA h g}_{\text{composite}}^{-1}$ was obtained after 100 cycles.

To understand the reason of the improved electrochemical performance of the Li/CPE/S cell, morphology of two different sides of the composite electrolyte after a few cycles was investigated by SEM equipped with an energy-dispersive X-ray (EDX) spectroscopy.

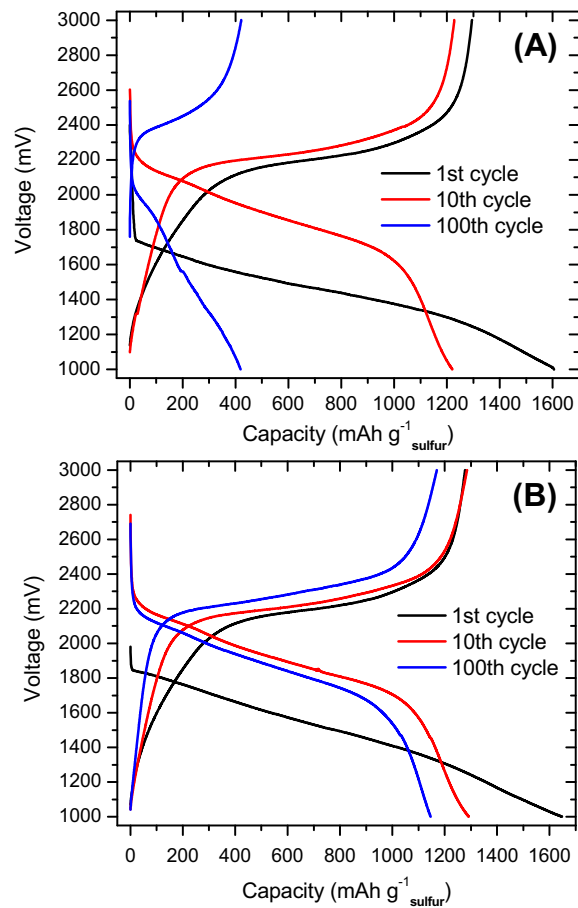


Fig. 5. Charge/discharge curves of (A) Li/liquid electrolyte/S and (B) Li/CPE/S battery cells at 0.2 C.

Measuring the amount of sulfur deposited on the surface of either electrolyte or lithium metal can be considered a powerful tool to determine active mass loss during cycling. After opening the cell, we did not observe any electrolyte solution in the battery indicating the ability of the electrolyte membrane to uphold the solution during cycling. Also, there was no agglomeration phase on the lithium metal surface. SEM images for the two different sides of composite electrolyte together with the EDX signals and S mapping

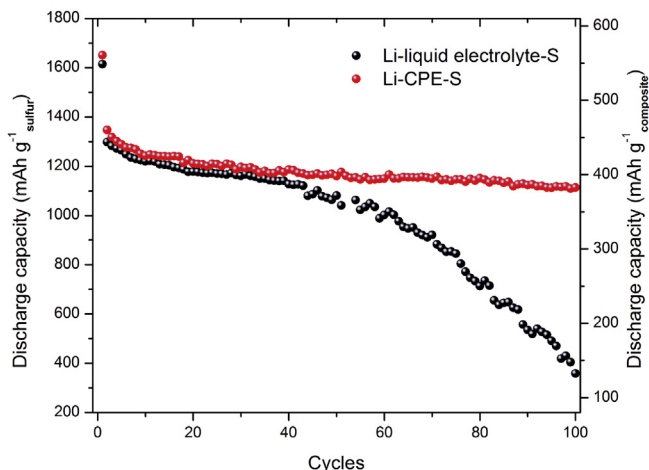


Fig. 6. Discharge capacity versus cycles of the battery cells at 0.2 C rate.

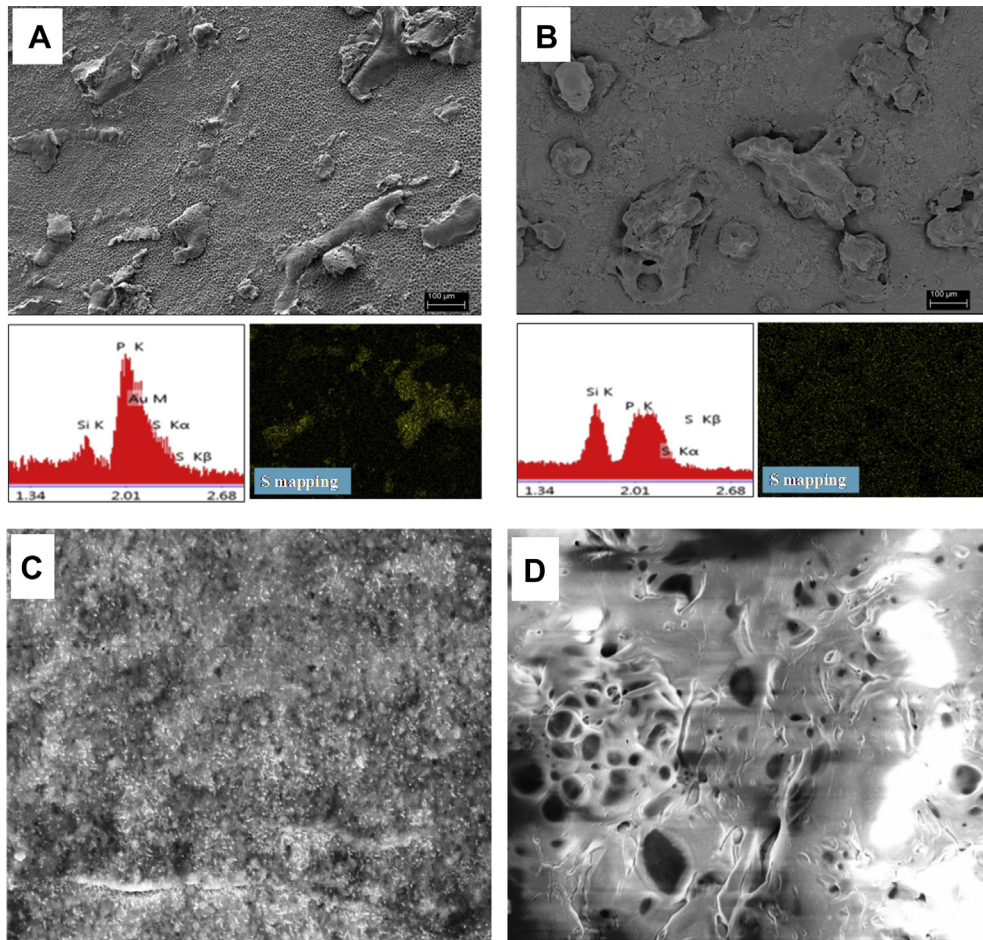


Fig. 7. SEM and EDX results for two sides of the composite electrolyte after 25 cycles. (A) The side in contact with sulfur-based cathode, and (B) the side in contact with lithium metal. Scale bar = 100 μm , (C) and (D) SEM images of fresh lithium metal, and lithium metal after cycling.

are shown in Fig. 7. Atomic amount of S in Fig. 7(A) is 1.38%, while this value in Fig. 7(B) is 0.03%.

It seems that physical immobilization of the liquid electrolyte solution within the composite membrane containing mesoporous particles can promote the electrolyte uphold and retard dissolution of polysulfides during cycling. Also, the migration of generated polysulfides through the electrolyte membrane is effectively hindered to suppress the shuttle phenomenon. The combination of these effects leads to achieving such a high and stable capacity for the Li/S battery cell after a long cycling.

4. Conclusions

A novel composite polymer electrolyte based on polymer matrix and mesoporous silica particles was prepared and used in high performance Li/S batteries. Mesoporous silica particles were synthesized by a simple procedure. The resultant composite electrolyte displayed exceptional electrochemical properties of low ohmic resistance and relatively high charge transfer resistance, indicating the ease of Li^+ ion transportation and suppression of polysulfide shuttling between lithium anode and sulfur-based cathode. As a result, a high and stable discharge capacity of 1143 mA h g^{-1} was obtained after more than 100 cycles.

Acknowledgments

This research was financially supported by Positec, the Natural Sciences and Engineering Research Council of Canada (NSERC),

Canadian Foundation for Innovation (CFI) and the Canada Research Chairs (CRC) program.

References

- [1] C. Barchasz, F. Mesquich, J. Dijon, J.C. Lepretre, S. Patoux, F. Alloin, *J. Power Sources* 211 (2012) 19–26.
- [2] H.S. Ryu, J.W. Park, J. Park, J.P. Ahn, K.W. Kim, J.H. Ahn, T.H. Nam, G. Wang, H.J. Ahn, *J. Mater. Chem. A* 1 (2013) 1573–1578.
- [3] Y. Yang, G. Yu, J.J. Cha, H. Wu, M. Vosgueritchian, Y. Yao, Z. Bao, Y. Cui, *ACS Nano* 5 (2011) 9187–9193.
- [4] J. Guo, Y. Xu, C. Wang, *Nano Lett.* 11 (2011) 4288–4294.
- [5] L. Yin, L. Wang, X. Yu, C.W. Monroe, Y.N. Li, J. Yang, *Chem. Commun.* 48 (2012) 7868–7870.
- [6] Y.V. Mikhaylik, J.R. Akridge, *J. Electrochem. Soc.* 151 (2004) A1969–A1976.
- [7] C.S. Kim, A. Guerfi, P. Hovington, J. Trottier, C. Gagnon, F. Baray, A. Vijh, M. Armand, K. Zaghib, *Electrochim. Commun.* 32 (2013) 35–38.
- [8] Y. Fu, A. Manthiram, *Chem. Mater.* 24 (2012) 3081–3087.
- [9] L. Xiao, Y. Cao, J. Xiao, B. Schwenzler, M.H. Engelhard, L.V. Saraf, Z. Nie, G.J. Exarhos, J. Liu, *Adv. Mater.* 24 (2012) 1176–1181.
- [10] J. Hassoun, B. Scrosati, *Adv. Mater.* 22 (2010) 5198–5201.
- [11] X. Liang, Z. Wen, Y. Liu, M. Wu, J. Jin, H. Zhang, X. Wu, *J. Power Sources* 196 (2011) 9839–9843.
- [12] L. Wang, X. He, X. Li, M. Chen, J. Gao, C. Jiang, *Electrochim. Acta* 72 (2012) 114–119.
- [13] J. Gao, M.A. Lowe, Y. Kiya, H.D. Abruna, *J. Phys. Chem. C* 115 (2011) 25132–25137.
- [14] A.M. Stephan, K.S. Nahm, *Polymer* 47 (2006) 5952–5964.
- [15] J. Wang, L. Liu, Z. Ling, J. Yang, C. Wan, C. Jiang, *Electrochim. Acta* 48 (2003) 1861–1867.
- [16] X. Ji, S. Evers, R. Black, L.F. Nazar, *Nat. Commun.* 2 (2011) 325–332.
- [17] K. Jreddi, M. Ghaznavi, P. Chen, *J. Mater. Chem. A* 1 (2013) 2769–2772.
- [18] K. Jreddi, Y. Zhao, Y. Zhang, A. Konarov, P. Chen, *J. Electrochem. Soc.* 160 (2013) A1052–A1060.

- [19] J.H. Lei, D. Liu, L.P. Guo, X.M. Yan, H. Tong, *J. Sol.-Gel Sci. Technol.* 39 (2006) 169–174.
- [20] J. Wang, J. Yang, C. Wan, K. Du, J. Xie, N. Xu, *Adv. Funct. Mater.* 13 (2003) 487–492.
- [21] X.G. Yu, J.Y. Xie, J. Yang, H.J. Huang, K. Wang, Z.S. Wen, *J. Electroanal. Chem.* 573 (2004) 121–128.
- [22] T.N.L. Doan, M. Ghaznavi, Y. Zhao, Y. Zhang, A. Konarov, M. Sadhu, R. Tangirala, P. Chen, *J. Power Sources* 241 (2013) 61–69.
- [23] L. Wang, X. He, J. Li, J. Gao, J. Guo, C. Jiang, C. Wan, *J. Mater. Chem.* 22 (2012) 22077–22081.
- [24] J. Fanous, M. Wegner, J. Grimminger, A. Andresen, M.R. Buchmeiser, *Chem. Mater.* 23 (2011) 5024–5028.
- [25] S.S. Jeong, Y.T. Lim, Y.J. Choi, G.B. Cho, K.W. Kim, H.J. Ahn, K.K. Cho, *J. Power Sources* 174 (2007) 745–750.